euspen's 25th International Conference & Exhibition, Zaragoza, ES, June 2025
www.euspen.eu

Study on the effect of surface asperities on copper-copper electric contacts

Francesco Rasetti[1], Giuliano Bissacco[1]

[1]*Technical University of Denmark, Department of Mechanical and Civil Engineering, Building 425, 2800 Kongens Lyngby, DK*

frara@dtu.dk

Abstract
Electric contact resistance (ECR) is an undesired effect of electrical contacts between copper conductors, that is highly influenced by the morphology of the surfaces in contact. The management of ECR is particularly important when high currents are involved, as is the case for magnet wires for high power electrical machines. Joule heating in the wires, which is proportional to total resistance, is in fact among the main causes of malfunction and lifecycle reduction in electric machines. The objective of this study is to identify the influence of contact conditions of real surfaces on the electric contact resistance between copper conductors for high current electric motor applications. Through a combination of experimental contact resistance measurements and FEM simulations of loaded contact between measured surfaces and a rigid body, this study shows that the contact resistance depends on the real contact area while coupling to the externally applied load is removed when plastic deformation at the contact surface is achieved.

Surface; Resistance; Profile

1. Introduction

Electrification of the transport sector is among the main strategies for reduction of greenhouse gas emissions [1]. Rise in performance requirements for electric motors, including deployable power density (kW/kg) [2] and efficiency over a wide range of speeds [3], has led to considerable research effort to improve electrical and mechanical machine design. Hairpin windings technology, where classic stranded wires are substituted by thicker rectangular conductors, has quickly established itself as dominant winding technology for high performance motors, due to the higher slot fill factor and deterministic positioning in the windings enabling higher torque density, easier automation of the production line and minimization of copper losses [4]. Hairpins are constituted by rectangular section insulated wire formed into U-shape inserted into the lamination stack according to the prescribed winding arrangement. To close the circuit, the open ends of the wires are twisted and joined through laser welding. Twisting and connecting are the most critical steps of hairpin production process, both in terms of production quality and cost [5,6]. The permanent joints obtained from laser welding are reliable and durable but are not reversible so that conductors cannot be separated, and the disassembly of the lamination stack is no longer possible, thereby hindering maintenance, reusability and recycling of motor components. Reversible wire connections would allow easier assembling of the winding arrangement, quick dismantling of the connections, maintenance and end-of-life operations on the lamination stack. The main drawback is the onset of additional electric contact resistance (ECR) between the joined surfaces. ECR represents the unwanted effect of introducing a discontinuity in an electric circuit, yielding additional resistance and hence extra heat generation in the circuit [7]. ECR is a function of all contact conditions, principally contact pressure (p), area (A), and temperature (T). Biele et al. [8,9] evaluated the effects of pressure and temperature on copper connections for joined electrodes in resistance welding, providing experimental qualitative relations between contact resistance and surface characteristics, such as roughness and oxidation layer.

The present work combines an experimental investigation of the effect of surface morphology and plasticization under load on the evolution of contact topography of motor hairpin wires with a numeric simulation of real contact surface to investigate the real role of pressure and contact area on ECR. The objective is to provide a explanation for the behaviour of flat wire contacts and to correlate it with experimental ECR findings. The work is organized as follows. Section 2 contains a brief description of the experimental setup and test procedure used for determination of contact resistance. In Section 3, experimental results are presented and discussed. In Section 4 the computational model is presented. In Section 5 the findings from the simulations are presented and their relevance towards explaining the experimental behaviour is highlighted.

2. Materials and Methods

2.1. Experimental Procedure

The tested samples were Cu-ETP motor wires with 99.95% pure copper core with a double insulation layer of enamel and PEEK. The outer wire section is 3.9x1.95 mm, while the double insulation layer has a depth of 60 µm. The samples were cut to measure and the insulation was stripped only at the ends to prevent short circuiting at the interfaces. The contact surface for each specimen was then prepared on a grinding wheel to ensure uniformity of surface topography. An Alicona G4 InfiniteFocus optical microscope is used to scan the surface before and after mechanical testing.

The test setup (Fig. 1) was built on an Instron-5965 vertical press with 5kN maximum compression load. The load is measured through a 1kN calibrated load cell placed on the moving truss of the press. The tested sample is fixed vertically on an aluminium bridge support, while a second wire is blocked horizontally on the fixed press bottom layer. The wires are loaded incrementally between 5N and 200N, with 5N steps and a waiting time of 1 minute at each load increment, both in

loading and unloading. Contact resistance is measured throughout the test.

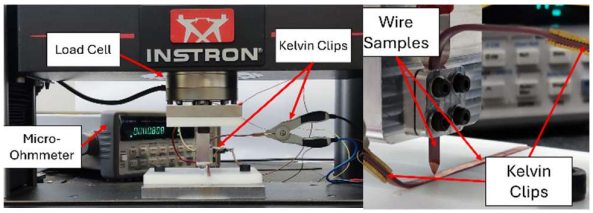

Figure 1. Experimental setup.

The measure of resistance is possible through a Four Wire Measurement array, where a current generator and a voltmeter are connected to the measurand to compensate the effect of the circuit [10]. A Keysight 34420A Micro Ohmmeter with 1μΩ resolution is used both as current generator and measurement device for circuit resistance. Kelvin Clips are applied on the hairpin wires' ends to close contact in the circuit, with application of compression springs. The reading of the Ohmmeter (R_Ω) is the sum of three different resistance components: contact resistance at the wires' interface (ERC), material resistance of the copper wire (R_{mat}) and contact resistance between the Kelvin Clips and samples (R_{probe}). To isolate the effect of ERC between the wires, the effect of material and probes must be quantified and removed from the reading.

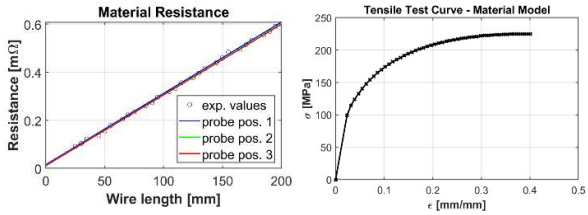

Figure 2. Material properties: (a) material and probe resistance curves, (b) engineering stress-strain curve for wire material

To assess the value of material resistivity ρ and probe contact resistance, solid wire strips of defined lengths were cut, stripped and their resistance was measured. For each sample, the value of R_Ω was found at three different probes' positions. The curve in Fig.2a summarizes the findings for both material and probe contact resistance. The angular coefficient of the curves represents the resistance of the material per unit length (R_L[Ω/m]), while the intercept at the y-axis is 2*R_{probe}.

Once the value of R_L is known, material resistivity, and consequently material resistance for the wire, can be estimated:

$$\rho = R_L \cdot A \quad (1)$$

Once material and probe resistance components have been found, the value of contact resistance is:

$$ERC = R_\Omega - R_{mat} - 2 \cdot R_{probe} \quad (2)$$

3. Contact Resistance in EV windings

ECR is a complex phenomenon, and it is affected by the conditions at which the contact happens. The morphology of the contact at the microscale and the elastoplastic deformations of the surface asperities under load determine the real contact area and the average contact pressure.

Fig.3 shows two curves describing the evolution of contact resistance upon loading and unloading for two samples, one having a pyramidal shape, thus characterized by restricted contact area, and undergoing significant plastic deformation upon loading. The other one having a nominally flat surface, with no apparent contact area restriction, showing no macroscopic plastic deformation after the test. The behaviour of the two samples is similar in loading, but very different upon unloading. While the flat sample, shows similar behaviour between loading and unloading, with a clear coupling between load and contact resistance, with higher loads yielding a reduction of ECR, for the pyramidal sample the loading curve is similar to the flat sample, while upon unloading ECR remains low until almost all the load is removed.

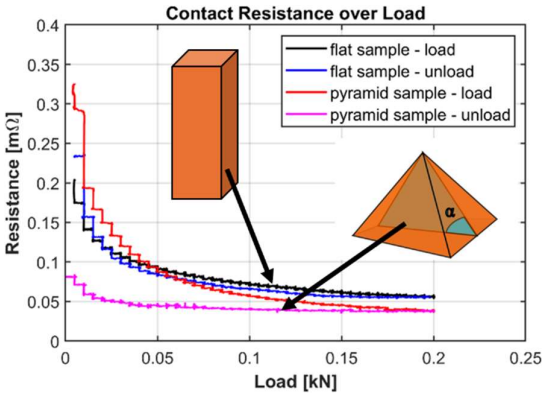

Figure 3. Load and unload curves for flat and pyramid sample

The main difference between the two curves is the ratio between apparent (A_a) and real (A_r) contact area in the junction. For the pyramidal sample, due to plastic deformation at the tip, $A_a \approx A_r$, while for the flat sample the contact surface A_r where current flows is only a small portion of the macroscopic cross section. In this case, the contact happens only through the interaction of microscopic roughness peaks at the interface. Understanding the behaviour of flat samples and the evolution of the contact upon load and unload requires therefore an in-depth analysis of the topographic features of the surface. Plastic deformation of roughness peaks plays in fact an important role in the determination of contact conditions.

3.1. Contact Resistance of flat winding ends

To assess the behaviour of rough surfaces in elasto-plastic contacts, it is necessary to understand the evolution of the microscopic surface features at the interface. In fact, while the macroscopic topology of the sample remains unaltered, plasticization still happens at lower scales. Both behaviours can be seen when analysing the surface of a flat sample before and after a test. The analysis of surface topography shows asperities flattening compatible with local plasticization of peaks in contact. The low-scale plasticization also explains the slight hysteretic behaviour of the ECR curve for the flat sample at the higher loads (Fig.3), where the unloading curve does not fully follow the behaviour in loading conditions, as one would expect in case of perfect elastic contact. Instead, a decrease in contact resistance is observed for the sample, compatible with a residual plasticization in localized contact regions.

The main limitation for the assessment of contact conditions through optical microscopy is that the surface can be analyzed only once the load has been completely removed, and hence the elastic component of the real contact is lost. On the other end, Finite Elements simulation of the contact interaction yields an estimate of the evolution of the surface at a microscopic level, and allows to define the elastic contact during the load cycle.

4. Rough surface contact simulations

Modelling rough surface contacts through finite elements is a challenging effort due to both the high computational effort

required to capture small topological features in a surface span that is technically relevant, and to the large plastic deformation that roughness peaks undergo when contact is established. Even at low load levels, the real contact area for roughness peaks is so little that the resulting stress is extremely high. This in turn means that the material model for the elements at the interface needs to take into account the heavy plasticization that the elements undergo. Appropriate contact and boundary conditions also need to be set to simulate surface behaviour.

4.1. Material Model for Simulations

When modelling contacts between rough surfaces, high deformations must be expected for elements close to contact area even when the macroscopic contact can be considered elastic. An appropriate material behaviour beyond elastic regime should hence be defined to take into account plasticization phenomena occurring at the interface, especially when the contact area is small enough for nodal load to approach UTS, so as not to incur in convergence issues. An elasto-plastic material model has been defined for the phenomenological simulation of the interaction, neglecting crystal plasticity effects. The material stress-strain curve in Fig.2b was built from repeated tensile testing on copper specimens, and it represents the behaviour of the wires under uniaxial tensile loading. The curve was integrated in the Finite Elements model as a multilinear material model. For the present analysis, the effect of strain rate is not considered, as the interaction is simulated in static conditions.

4.2. Computational Problem Definition

The main assumptions and conditions for the model are here presented. The true morphology of the contact surfaces used in the experimental tests described in Section 3.1 was obtained by performing surface measurements using an Alicona G4 focus profilometer with 20X magnification, achieving a point interval of 2 µm in X and Y directions and a resolution of 100 nm in Z direction. A very fine mesh size was used close to the contact surface to capture the smallest wavelength of asperities. The characteristic size of undeformed elements was chosen to be $dl \leq 2$ µm, so as not to lose quality upon meshing.

A thick material substrate is also necessary to avoid excessive macroscopic deformation and to guarantee homogeneous load distribution in material bulk. Hence, to reduce the amount of elements in the analysis, element size is progressively increased as the distance from the contact surface increases. Even so, the number of elements is extremely high, especially when considering relatively large domains (Fig.4).

The contact was modelled, using a well-established convention [11], as an elasto-plastic deformable rough body, with periodic symmetry constraints in x and y directions, in contact with a rigid flat plane. The Rough Contact hypothesis assumes an infinite friction coefficient at the interface, thereby ensuring no sliding between the interacting surfaces. The elasto-plastic rough body was loaded in compression at rising values of pressure in the z direction, while the rigid body was kept still.

5. Results

By simulating the evolution of the microscopic features, the evolution of the contact can be studied both in terms of variation in the real contact area and of pressure on the interface points.

Four surfaces, sampled from the same tested specimen, have been considered for the numerical analysis. For the present study, only contacts of rough surfaces with flat planes have been considered, in order to minimize computational burden without loss of significance. The surfaces were tested upon complete load and unload cycle to better understand the hysteresis effect on contact resistance due to plasticization.

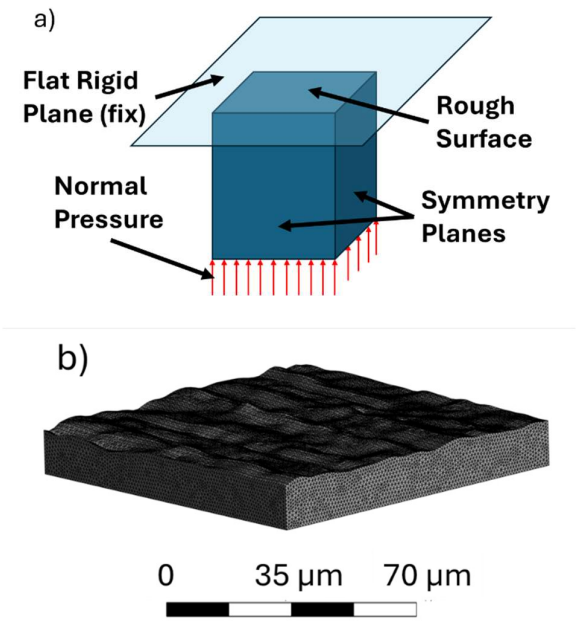

Figure 4. Description of the simulated system: a) schematic contact conditions description, b) example of meshed rough contact surface

Fig.5b-e provide a visual representation of the simulated surface before and after load application. The effect of the loading cycle can be clearly seen from the evolution of the surface profile, in particular the flattening of the peaks. The experimental surface behaviour in Fig.5a is very different from the one displayed in simulated surface interactions. This is due to the simplifying hypothesis of rigid body and plane surface for contact target. In real applications, both bodies in contact have rough surface topology, yielding complex peak-peak interactions instead of the simplified peak-plane flattening.

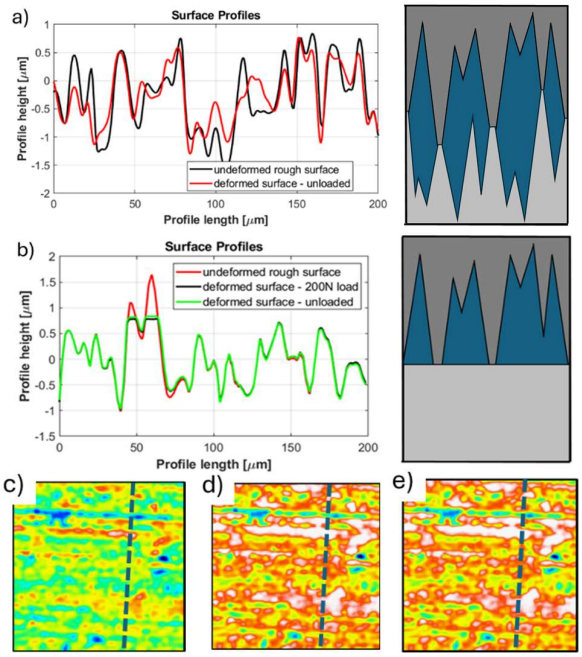

Figure 5. a) Experimental profile curves before and after rough-rough flat surface contact; b) Profile curves for numerical rough-smooth contact for c) undeformed surface, d) fully loaded deformed surface and e) unloaded deformed surface

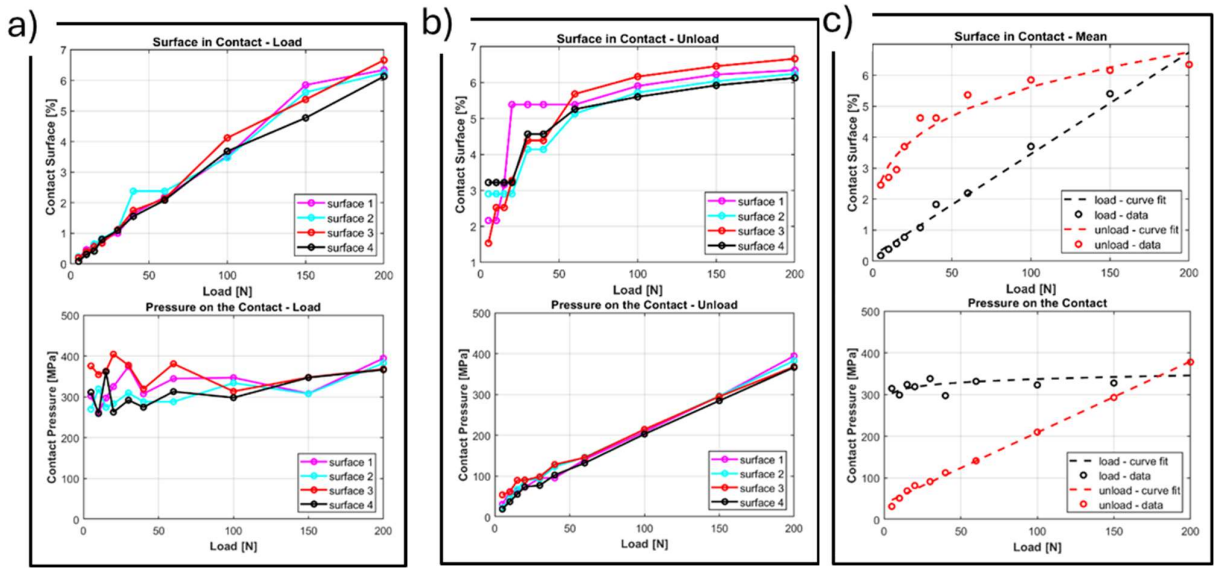

Figure 6. Result curves for simulated contact. Contact surface and pressure upon loading (a) and unloading (b), tendency of contact surface and pressure in load and unload (c).

Moreover, in the simulated scenario the plane is assumed to be completely undeformable, while in real copper-copper contacts asperities on both sides undergo plastic deformation.

The evolution of contact load and real contact area, which cannot be detected during the experimental study, can instead be tracked in the simulations. Thus the simulations are helpful in understanding the evoulution of the contact conditions. In Fig.6 a quantitative representation of real contact surface and contact pressure is given for load and unload sequences.

Fig.6a shows a linear trend for the area of contact as the load increases, while the pressure at the contact instantly rises at contact onset and remains at approximately constant values in the range of 300-400MPa regardless of the increasing load. Upon unloading (Fig.6b), while the contact area decreases slowly until it plummets at low load levels (F<50N), the pressure follows a linear descending tendency, compatible with fully elastic contact of the plasticized surface. The results in Fig. 6 show that all four simulated surface patches behave in identical ways with respect to pressure and real contact area evolution and effects related to local contact morphology are disregarded. This is a consequence of the introduction of a perfectly flat rigid body as the counter surface.

5. Conclusions and Future Work

The present work aimed at furthering the understanding of the impact of surface topography on the value of contact resistance in elastoplastic contact between rough bodies. Finite element modelling of real surface specimens has been used to analyze the evolution of contact conditions along a load-unload experimental cycle. The findings show that upon loading the pressure load remains almost constant while the contact area grows linearly. Upon unloading instead the contact area remains constant until the load drops below 50MPa and then drops rapidly, while contact pressure decreases linearly with the load.

Despite the simplifications introduced, elastoplastic contact simulations enable monitoring the real contact area and contact pressure under varying loading and provide an explanation of the effect of plasticization on the behavior of rough copper-copper contacts that can be used for the feasibility assessment and design of reversible low-resistance hairpin junctions.

Future work will focus on establishing a direct dependency between surface preparation and final ECR curve through numerical modelling, and minimizing contact resistance through shape and topography design to have minimal contact thermal losses in motor windings.

6. Acknowldgements

This research has received funding from the EU's Horizon Europe research and innovation program EU MSCA DN under grant agreement no. 101072580, HIPO: Integrated high-speed power systems for industry and mobile applications. The content of this publication does not reflect the official opinion of the EU.Responsibility for the information and views expressed in the publication lies entirely with the authors.

References

[1] European Commission White Paper 2011 'Roadmap to a Single European Transport Area – Towards a competitive and resource efficient transport system'

[2] Zhang F. et al. 2021 *IEEE Transaction on Transportation Electrification* **7** 2914-2926

[3] Gerada D. et al. 2014 *IEEE Transactions on Industrial Electronics* **61** 2946-2959

[4] Bianchi N. and Berardi G. 2018 *IEEE Energy Conversion Congress and Exposition (ECCE)* 4398-4405

[5] Hausmann L., Wirth F. and Fleischer J. 2022 *International Electric Drives Production Conference (EDPC)*

[6] Glaessel T., Seefried J., Franke J. 2017 *International Electric Drives Production Conference (EDPC)*

[7] Holm R. 1946 'Electric Contacts: Theory and Applications' (Springer-Verlag Berlin Heidelberg)

[8] Biele L., Schaaf P. and Schmidt F. 2021 *Phys. Status Solidi A* **218**

[9] Biele L., Schaaf P. and Schmidt F. 2022 *IEEE Transactions on Components, Packaging And Manufacturing Technology* **12** 973-980

[10] Keithley Instruments Inc. 2004 'Low Level Measurements Handbook' (Cleveland OH)

[11] Barber J.R. 2003 Proc. R. Soc. Lond. *A* **459** 53-66